August 27-31, 2023
FLORENCE - ITALY
ICWE 16
16th International Conference on Wind Engineering

Wave-induced wind turbulence – experimental results of combined wind and wave conditions in a Norwegian fjord

Jungao Wang [1,2], Guy L. Larose [3], Bernardo Costa [4]

[1]*Norwegian Public Roads Administration, Stavanger, Norway, jungao.wang@vegvesen.no*
[2]*Department of Mechanical and Structural Engineering and Materials Science, University of Stavanger, Stavanger, Norway*
[3] *RWDI Inc., Ottawa, Ontario, Canada, guy.larose@rwdi.com*
[4]*Norwegian Public Roads Administration, Stavanger, Norway, bercos@vegvesen.no*

SUMMARY:
Experimental studies of combined wind and wave conditions in a Norwegian fjord were presented. The studies were conducted to investigate if additional wind turbulence would be induced by waves when in proximity to the wave surface. Boundary layer wind flow and waves were generated simultaneously in a wind-wave test facility to simulate strong wind and wave conditions. Wind turbulence was measured at four different heights. Testing categories including wind only, wind with regular waves and wind with irregular waves were designed to study the wind-wave interactions. Additional wave-induced spectral peaks were clearly observed in the vertical turbulence spectra and were more distinct in the regular wave cases. Further analysis indicated that the additional wave-induced wind turbulence had an exponential decaying trend with increasing height. An empirical formula was proposed with parameters fitted to the experimental data, providing a basis to consider extra wind turbulence for the bridge design.

Keywords: wind-wave interaction; marine atmospheric boundary layer; wind tunnel tests.

1. INTRODUCTION

The Norwegian Public Roads Administration is developing a 5 km long floating bridge crossing Bjørnafjorden in southwestern Norway (Vegvesen, 2018). It is proposed that the bridge girder be supported by several floating pontoons and would be relatively close to the water surface (ca. 16 m) for most of its length. The influence of the waves on the turbulence of the approaching winds near the water surface was investigated at the Extreme Air Sea Interaction facility, University of Melbourne. This facility consists of an open return blower wind tunnel that is built over a wave tank with a working section of 60 x 1.8 x 2 m (length x width x height). In this study, the water depth was set to be 0.87 m, leaving an effective wind tunnel working section height of 1.13 m. Figure 1 shows the schematic of the wind-wave test facility, indicating the measurement location 23 m downstream of the working section inlet. The geometrical scaling ratio of the experiments was chosen to be 1:30 based on the dimensions of the testing facility, the capacity of the wave paddle and the maximum wind speed. The tested wind and wave conditions were selected to be representative of the design cases and the strong wind and wave events monitored through long term field measurement campaign in Bjørnafjorden (Vegvesen, 2022).
The model test consisted of 1) wind only cases; 2) wind combined with regular wave cases; and 3)

wind combined with irregular wave cases. The wave height of the regular wave cases was selected to be about 1.5 times the significant wave height of the corresponding irregular wave cases and the wave period was chosen to be the same as the irregular wave cases.

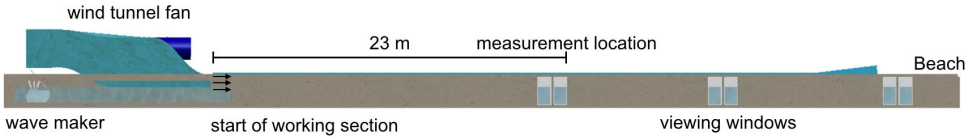

Figure 1. Schematic drawing of the Extreme Air Sea Interaction facility of the University of Melbourne, highlighting its main features.

The airflow measurements were taken using 4 Cobra probes. As shown in Figure 2, these probes were held by aerofoil-shaped mount at 4 locations corresponding to full-scale elevations of 7, 10, 13 and 16 m. Three ultrasonic sensors were used to measure the wave elevations. The sampling frequency was set at 1000 Hz and each test case had a sampling duration of about 1 hour in full-scale, divided into 10 independent segments to avoid the undesirable effect of wave reflection.
Air flow with low turbulence intensity was generated at the inlet of the working section, and a boundary layer flow was formed along the free water surface. The relatively low background turbulence level was not intended to match the actual turbulence level at the fjord in these experiments. It was assumed that any additional wave-induced wind turbulence would not be significantly affected by the background turbulence. Figure 3 presents the target and measured mean wind speed and turbulence intensities of 3 repeated runs under irregular waves generated for an equivalent full-scale return period of 100 years, based on the recommendations in N400 (Vegdirektoratet, 2022). The generated turbulence intensities are lower than the targets, considering a shorter fetch and smooth wind condition at the wind tunnel inlet. As for the waves, no short-crested waves (as observed in the fjord) were generated due to the limitation of the facility, however, the irregular waves are simulated to match the Jonswap wave spectra.

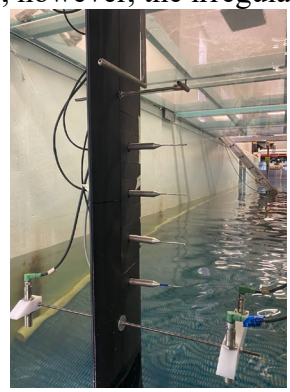

Figure 2. Cobra probes and wave sensors configurations used in this study.

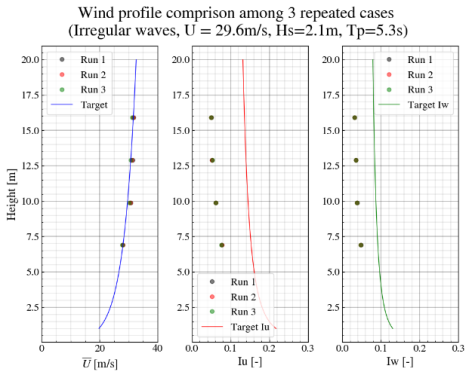

Figure 3. Wind profile comparison for irregular waves among 3 repeated cases (100-year return period).

2. EXPERIMENTAL RESULTS

Figure 4 (a) presents the power spectral densities (PSDs) of along-wind and vertical turbulence and wave elevations for the combined wind and irregular wave conditions, with a return period of 100 years. A shaded area is highlighted in the spectral plots, corresponding to the frequency range in which the wave energy concentrated. This is the range of interest for additional wind turbulence due to the waves. Additional turbulence was revealed in the vertical wind spectra and these spectral peaks resemble the shape of the wave spectrum S_{fh}. It is, however, difficult to depict similar

additional spectral peaks in the along-wind wind spectra, partly due to the relatively stronger background turbulence of the along-wind flow component. As expected, the additional vertical wind turbulence due to waves appeared to decay with the increasing height. Figure 4 (b) presents the wind turbulence PSDs of 3 repeated irregular wave cases in a broader frequency range, with distinct additional spectral peaks in the vertical wind spectra. Apart from this additional spectral peak, the remaining spectral shape was found to be similar to the pure wind cases. Based on this, smoothed background wind spectra were reconstructed by bin-averaging, together with a linear fitting within the frequency range of the additional spectral peak. By subtracting the smoothed background wind spectra from the original measured spectra, the additional wind spectra due to waves can be extracted, as illustrated by the green curves in Figure 4 (c). The variances of the observed additional turbulence were calculated by integrating the separated spectra over the highlighted frequency range.

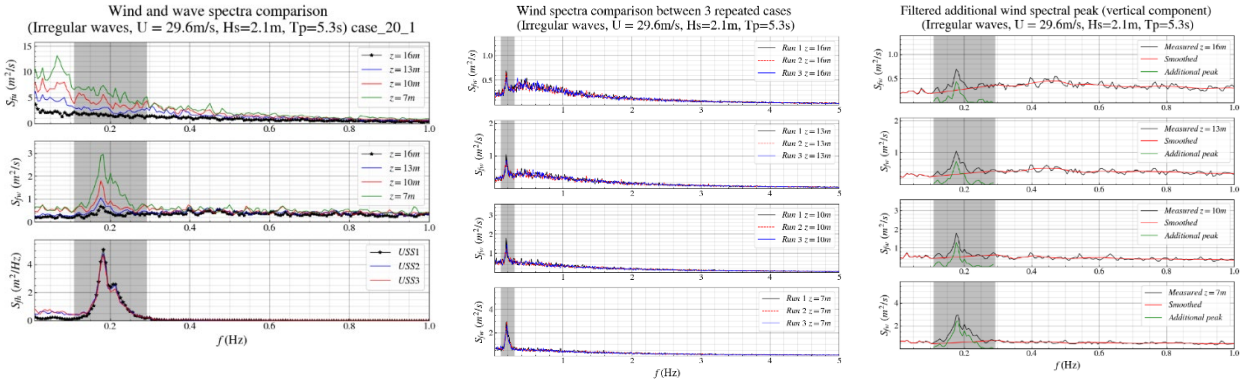

(a) (b) (c)

Figure 4. Wind and wave spectra in irregular waves (100-yr return period). (a) PSDs of the along-wind and vertical turbulence and of the wave elevation; (b) PSDs of the vertical turbulence at 4 heights; (c) measured and filtered additional vertical wind spectra due to the presence of the waves.

Figure 5 presents results for the regular wave cases. For these cases, the additional wave-induced spectral peaks were found to be clearly revealed.

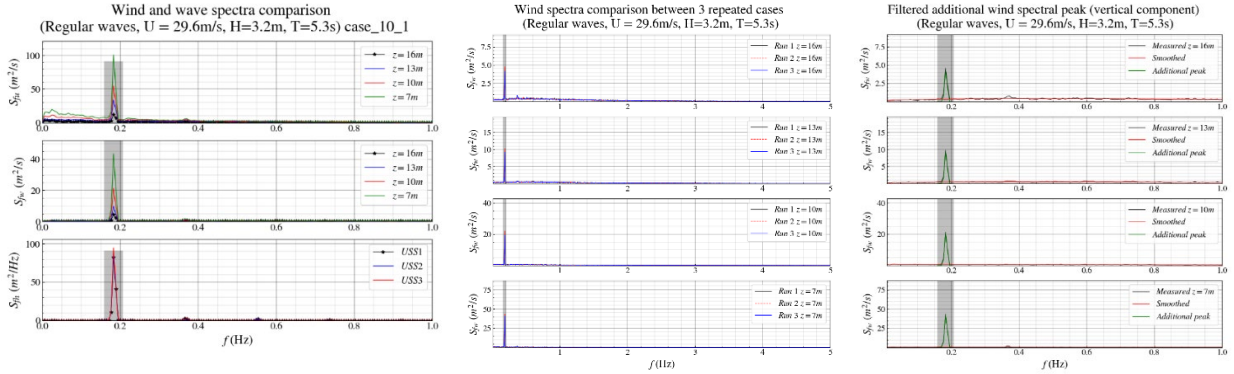

(a) (b) (c)

Figure 5. Wind and wave spectra in regular waves (100-yr return period). (a) PSDs of the along-wind and vertical turbulence and of the wave elevation; (b) PSDs of the vertical turbulence at 4 heights; (c) measured and filtered additional vertical wind spectra due to the presence of the waves.

Based on all test cases, empirical formulas can be fitted to characterise the additional wind turbulence due to the waves. The following empirical formulation proposed by Kitaigorodskii et al. (1983) was used to fit the experimental data:

$$\frac{\sigma_{i\_wave}}{\sigma_{wave} * \omega_p} = A_i * \exp\left(-B_i * k_p * z\right); i = u, w \quad (1)$$

where, σ_{i_wave} is the standard deviation of the additional wind turbulence, σ_{wave} is the standard deviation of the wave elevation; ω_p is the (peak) wave frequency in radians; k_p is the wave number; z is the height at which the wind turbulence is considered; and, A_i and B_i are two empirical parameters to be fitted.

Figure 6 presents the results for all irregular wave cases. The results for design cases under 3 different return periods at the potential elevation of the floating bridge (16 m) are highlighted by different coloured markers. The results for different combination of wind and waves were found to be roughly organised. The fitted empirical curve shown in Figure 6 (values of fitted empirical parameters reported in the legend) was selected to envelope the experimental data, with y-axis values above all experimental results, to stay on the conservative side.

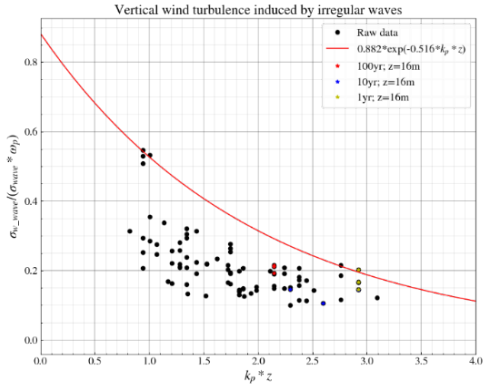

Figure 6. Fitted additional vertical wind turbulence due to waves (based on all irregular wave cases).

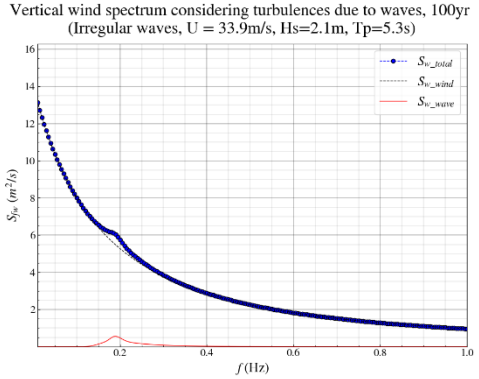

Figure 7. Example of reconstructed wind spectrum considering wave effects for 100-year return period.

Based on the above experimental observations, the standard deviation of the additional wave-induced wind turbulence can be estimated by Eq. (1) and the fitted parameters of Figure 6. With the assumption that the wave-induced wind turbulence has a spectral shape similar to the spectral shape of the waves (as it has been observed), the wave-induced wind spectra can be expressed by:

$$S_{i\_wave}(f) = {\sigma_{i\_wave}}^2 / {\sigma_{wave}}^2 * S_{wave}(f); i = u, w \quad (2)$$

Figure 7 presents an example of a reconstructed total wind spectrum considering the wave-induced components based on the fitted results shown in Figure 6. The wave-induced vertical component is visible in the total spectrum, but with a relatively small magnitude for this case.

3. CONCLUSION

This study presented experimental results characterising potential wave-induced wind turbulence considering the environmental conditions expected in the Bjørnafjord, Norway. An empirical formula was proposed with fitted parameters based on the experimental data, which provides a basis to consider the additional wave-induced wind turbulence for the floating bridge design.

REFERENCES

Kitaigorodskii, S., Donelan, M., Lumley, J., Terray, E., 1983. Wave-turbulence interactions in the upper ocean. Part ii. statistical characteristics of wave and turbulent components of the random velocity field in the marine surface layer. Journal of Physical Oceanography 13, 1988-1999.

Vegdirektoratet, 2022. Bruprosjektering Håndbok N400.

Vegvesen, S., 2018. Design basis Bjørnafjorden.

Vegvesen, S., 2022. MetOcean Specification